

## Measurements of Resonant Electron Capture in Close H<sup>+</sup>-on-H Collisions\*

HERBERT F. HELBIG† AND EDGAR EVERHART

*Physics Department, The University of Connecticut, Storrs, Connecticut*

(Received 4 June 1965)

Differential measurements of the electron capture probability  $P_0$  are made for protons scattered from atomic hydrogen targets. The incident proton energy ranges from 150 keV down to 0.130 keV and the scattering angle is varied between 0.2° and 6.0°. Seven sharply resonant peaks of  $P_0$  are found, their location depending on both energy and angle. For example, when the scattering angle is held at 6° the peaks are found at 21, 3.9, 1.7, 0.90, 0.54, 0.36, and 0.19 keV, and when the energy is fixed at 0.250 keV, peaks are found at 0.7°, 1.4°, 2.6°, and 4.5°. In some cases the equivalent collision with deuterium, D<sup>+</sup>-D, is used to augment the range of the measurements. These data extend those reported by Lockwood and Everhart (1962) who studied this same phenomenon in H<sup>+</sup>-H collisions over a smaller range in energy and at fixed 3° scattering angle. Relative differential-cross-section data are presented also which show a change in slope with the onset of rainbow-angle scattering conditions.

### 1. INTRODUCTION

RESONANT-electron-capture measurements for the proton-atomic-hydrogen collision were first described by Lockwood and Everhart.<sup>1</sup> In that measurement, fast protons were passed through an atomic-hydrogen target gas, and occasionally there was a "close encounter" such that the incident particle was scattered through an angle of several degrees in a single collision. These scattered particles were analyzed individually to see whether or not they had captured the electron during the collision. The fraction of the scattered particles which emerged neutral from such a collision was termed  $P_0$ , the electron-capture probability. In this earlier work<sup>1</sup> the scattering angle was fixed at 3° and the energy range extended from 40 to about 0.7 keV. When  $P_0$  was plotted versus incident energy a sharply resonant structure was seen, with four peaks in the above-mentioned energy range.

The present study repeats these measurements and extends them to include the thousandfold energy range from 150 keV down to 0.130 keV. Furthermore, by varying the scattering angle between 0.2° and 6.0°, it is shown that  $P_0$  is a resonant function of scattering angle as well as of energy. The wide range in impact parameter and velocity represented by these data discloses seven peaks of  $P_0$ . In addition, relative differential-cross-section data are presented which show evidence of the influence of rainbow-angle scattering.

This study of the H<sup>+</sup>-H system is parallel to our recent experiments on resonant electron capture in the He<sup>+</sup>-He system<sup>2,3</sup> and on a similar phenomenon in the H<sup>+</sup>-He system.<sup>4</sup>

The impact-parameter method,<sup>5</sup> rather fully de-

veloped in the early 1950's, provided the first theoretical explanation of these resonances in  $P_0$ , although neither the locations nor the amplitudes were predicted correctly by the theory in its original form. Since then, Bates and McCarroll,<sup>6</sup> Bates and Williams,<sup>7</sup> Mukherjee and Sil,<sup>8</sup> and Fulton and Mittleman<sup>9</sup> have introduced refinements in the impact-parameter method which have resulted in somewhat improved agreement with the measurements.

A different approach to the charge-transfer problem has treated the nuclear motion by wave analysis. Thus, Francis J. Smith<sup>10</sup> and Felix T. Smith<sup>11,12</sup> have studied, respectively, the H<sup>+</sup>-H and He<sup>+</sup>-He systems using the method of partial waves. Roth<sup>13</sup> treated the nuclear motion as a Coulomb wave perturbed by the presence of the atomic electron. The present data will be compared with the predictions of these several theoretical results, and it will be seen that discrepancies yet exist.

### 2. THE EXPERIMENT

In these experiments a proton beam is passed through low-pressure hydrogen in a tungsten furnace which is maintained at a temperature of about 2600°K. Under these circumstances almost none of the hydrogen gas remains in molecular form. Collimating apertures select those particles which have been scattered through a small angle  $\theta$ . These scattered particles are analyzed electrostatically to determine their charge and are then

\* This work was supported by the U. S. Army Research Office, Durham, North Carolina.

† Now at Clarkson College of Technology, Potsdam, New York.

<sup>1</sup> G. J. Lockwood and E. Everhart, *Phys. Rev.* **125**, 567 (1962).

<sup>2</sup> G. J. Lockwood, H. F. Helbig, and E. Everhart, *Phys. Rev.* **132**, 2078 (1963).

<sup>3</sup> E. Everhart, *Phys. Rev.* **132**, 2083 (1963).

<sup>4</sup> H. F. Helbig and E. Everhart, *Phys. Rev.* **136**, A674 (1964).

<sup>5</sup> O. B. Firsov, *Zh. Eksperim. i. Teor. Fiz.* **21**, 1001 (1951);

T. Holstein, *J. Phys. Chem.* **56**, 832 (1952); D. R. Bates, H. S. W. Massey, and A. L. Stewart, *Proc. Roy. Soc. (London)* **A216**, 437 (1953).

<sup>6a</sup> D. R. Bates and R. McCarroll, *Proc. Roy. Soc. (London)* **A245**, 175 (1958).

<sup>6b</sup> D. R. Bates and R. McCarroll, *Advan. Phys.* **11**, 39 (1962); see Sec. 3.2, Eqs. (151)-(154) and Table 4, p. 75.

<sup>7</sup> D. R. Bates and D. A. Williams, *Proc. Phys. Soc. (London)* **83**, 425 (1964).

<sup>8</sup> S. C. Mukherjee and N. C. Sil, *Indian J. Phys.* **36**, 622 (1962).

<sup>9</sup> M. J. Fulton and M. H. Mittleman, *Bull. Am. Phys. Soc.* **10**, 129 (1965); University of California Radiation Lab Reports 7655 and 12251, 1964 (unpublished); *Ann. Phys. (N.Y.)* **33**, 65 (1965).

<sup>10</sup> Francis J. Smith, *Phys. Letters* **10**, 290 (1964); *Proc. Phys. Soc. (London)* **84**, 889 (1964).

<sup>11</sup> Felix T. Smith, *Bull. Am. Phys. Soc.* **9**, 411 (1964).

<sup>12</sup> R. P. Marchi and Felix T. Smith, *Phys. Rev.* **139**, A1025 (1965).

<sup>13</sup> B. Roth, *Phys. Rev.* **133**, A1257 (1964); **135**, AB1 (1964).

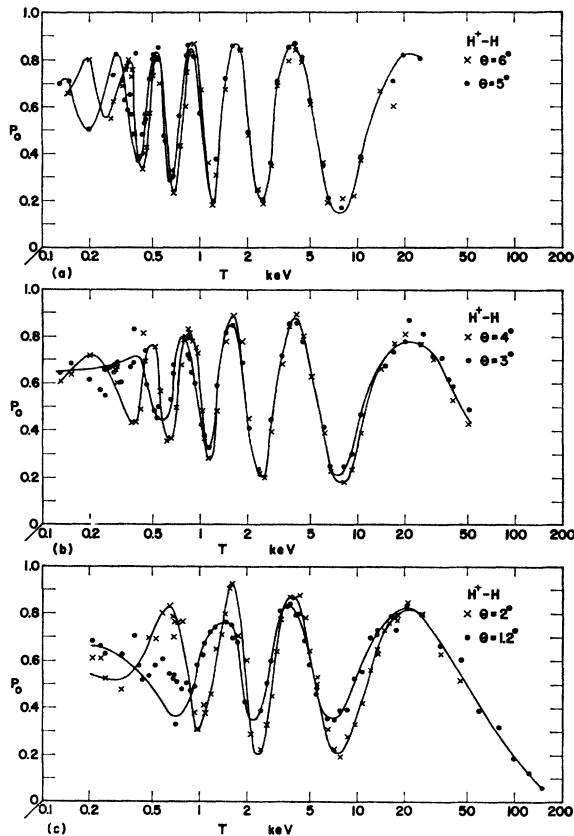


FIG. 1. The probability  $P_0$  for electron capture by protons colliding with hydrogen atoms is plotted versus incident-proton energy  $T$  in keV for several angles of scattering. The results shown for laboratory scattering angles  $\theta = 6^\circ, 5^\circ$ , and  $4^\circ$  are reduced from equivalent  $D^+D^+$  data, those for  $\theta = 3^\circ$  combine both the  $H^+H$  data and equivalent  $D^+D^+$  data, and the results for  $\theta = 2^\circ$  and  $1.2^\circ$  are obtained from  $H^+H$  data alone. Empirical lines are drawn through the data points.

counted. The apparatus is substantially the same as that previously described.<sup>1</sup>

#### a. Low Energies

The measurements of Lockwood and Everhart were terminated at 700 eV because of difficulties then encountered at lower energies in obtaining a sufficiently intense and stable proton beam from the University of Connecticut heavy-ion accelerator. A number of improvements in the distribution of potentials on the accelerator's focus electrodes and drift tubes, particularly operating some of the intermediate drift tubes at negative potentials, make possible the present use of proton or deuteron beams with energies down to about 200 eV.

#### b. Hydrogen and Deuterium

The design of the apparatus<sup>1</sup> restricts the scattering to angles no larger than  $3^\circ$ , and the  $H^+H$  data are taken down to a lower energy limit of 215 eV. To extend

these ranges, both the projectile and target gas are changed to deuterium. For small-angle atomic collisions a  $D^+D^+$  collision at angle  $\theta$  and energy  $T$  is the same in both velocity and distance of closest approach as an  $H^+H$  collision at  $2\theta$  and  $T/2$ . Thus  $D^+D^+$  data taken in the  $1^\circ$  to  $3^\circ$  region are equivalent to  $H^+H$  data taken between  $2^\circ$  and  $6^\circ$ . The lowest energy points, plotted at 130 eV are actually taken with  $D^+D^+$  at 260 eV. The  $H^+H$  and  $D^+D^+$  data, plotted in this way, are consistent.

#### c. Angular Measurements

The angular resolution has three effective values. The highest resolution  $H^+H$  data are taken in the angular range of  $0.2^\circ$ – $1.9^\circ$  with the collimating apertures small enough to yield an angular acceptance width  $2\Delta\theta$  of about  $0.14^\circ$ . (That is, 85% of the scattered particles detected are within  $\Delta\theta = \pm 0.07^\circ$  of the nominal scattering angle  $\theta$ .) The differential cross section drops so precipitously with angle that the collimating holes are made larger for most of the  $H^+H$  data, which are taken in the range of  $1.1^\circ$  to  $3^\circ$ . Here the angular acceptance width  $2\Delta\theta$  is about  $0.6^\circ$ . The  $D^+D^+$  data are actually taken with the same collimators. However, since the angular range of  $1^\circ$ – $3^\circ$  is doubled so as to plot equivalent  $H^+H$  data in the  $2^\circ$ – $6^\circ$  range, the corresponding value of  $2\Delta\theta$  is about  $1.2^\circ$  in this case.

Because of the rapid variation of differential cross section with angle, more particles arise from the region  $\theta - \Delta\theta$  than from the region  $\theta + \Delta\theta$ . Thus the center angle is slightly larger than the most probable scattering angle. This correction is made in those few cases where it is not negligible, and never exceeds  $0.1^\circ$ .

Although the incident beam is well-collimated, its measured direction is found to vary a few tenths of a degree according to the conditions of electrostatic and magnetic steering within the accelerator, furnace heating effects, and (at low energies) stray magnetic fields associated with the direct current which heats the furnace. This source of error in the scattering angle determination is largely eliminated by studying the scattering on both sides of the incident beam direction and choosing the zero index from the symmetry of the data curves.

#### d. Energy Measurements

At energies below a few keV it is not sufficiently accurate to find the energy of the ion beam from the voltage on the exit channel of the ion source. The ions are found to enter the scattering chamber with excess energies up to 100 eV, depending on the operating conditions of the rf ion source. (This phenomenon may be due to "plasma rectification" in the source.) For this reason the ion-beam energy is measured by deflecting the beam electrostatically in a calibrated device. The actual average beam energy is thus measurable to within 5 eV below 1000 eV. Although this correction

was made in the earlier work, the calibration is here improved and this makes small corrections to the energy values of the previously reported<sup>1</sup> peaks and valleys of  $P_0$  below 2 keV.

### e. Damping

The data to be presented show that the  $P_0$  oscillations do not extend from zero to unity. Such damping was not predicted by the impact-parameter-method theory in its earlier form, and it is thus important to discuss the precautions taken to ascertain whether the observed damping is due, in part, to experimental difficulties.

Any impurity in the target gas would have a much larger differential scattering cross section than atomic hydrogen and would be expected to display a significantly different electron capture dependence. Thus, small amounts of impurity in the target gas would cause disproportionately large damping effects. However, the target hydrogen gas, purported to be spectroscopically pure, is still further purified with cooled adsorbent traps. Such treatment does not change  $P_0$  and further, the data are reproducible despite changes in target gas containers. The evidence is that the target gas is adequately pure.

Damping would also be caused by the presence of undissociated (molecular) hydrogen in the target chamber.<sup>1</sup> In the present experiment the dissociation fraction is measured directly, using the method described by Lockwood, Helbig and Everhart,<sup>14</sup> and found to be greater than 95%. In addition it is found that further increase in furnace temperature does not change  $P_0$ .

The correct value of  $P_0$  can only be determined when the particles result from *single* collisions with the target atoms. This situation is ensured when the target gas density is low enough that  $P_0$  is not a function of density. The experiment is conducted under such conditions.

The detector is a second electron multiplier. The absolute heights of the  $P_0$  curves depend on the relative particle-counting efficiency (not the gain) for protons in comparison with neutral hydrogen atoms. The ions or atoms strike the multiplier's first dynode, which is grounded so that there is no post-acceleration of the scattered protons. At most times the multipliers are operated on a "plateau" where it is fairly certain that every particle, neutral or charged, is being counted.

The finite angular resolution causes a certain amount of damping at low energies as will be discussed in Sec. 3d, below. It is also possible that there is a systematic experimental effect, not now understood or allowed for, which would modify the damping of the oscillations as reported here.

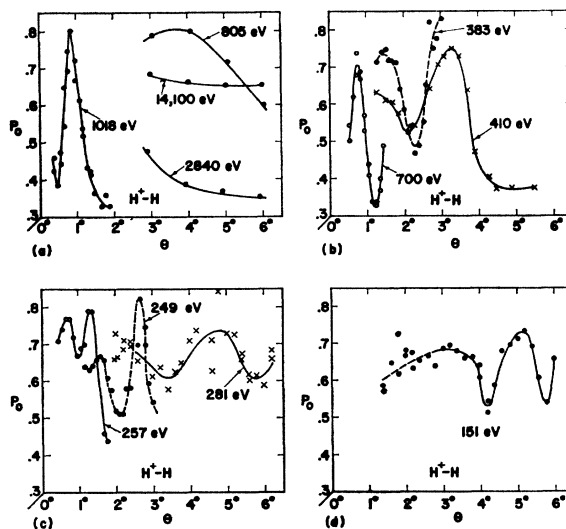


FIG. 2. Electron-capture probability  $P_0$  is plotted versus laboratory scattering angle  $\theta$  for collisions between atomic-hydrogen targets and protons whose energies are indicated. The data shown for energies 249, 257, 383, 700, and 1018 eV are obtained from  $H^+-H$  collisions, whereas the data shown at 151, 281, 410, 805, 2840, and 14 100 eV are obtained from equivalent  $D^+-D$  collisions. Three different effective angular resolutions are represented here as described in the text

### f. Procedure

In other respects the procedure and apparatus used for taking the data are the same as that previously described.<sup>1</sup>

## 3. DATA

The data show the dependence of  $P_0$  on the two experimental variables, incident-ion energy  $T$  and laboratory scattering angle  $\theta$ .

### a. Results

Figure 1 shows  $P_0$  versus  $T$  for scattering angles of  $1.2^\circ$ ,  $2^\circ$ ,  $3^\circ$ ,  $4^\circ$ ,  $5^\circ$ , and  $6^\circ$ . These curves are all in phase at high energies, but differ at low energies. The peaks are identified by integral values, and the valleys by half-integral values, of an index  $n$ , starting with  $n=1$  at the 21-keV peak, which is the highest energy peak. Figure 2 shows  $P_0$  versus  $\theta$  for representative energies between 14 100 and 151 eV. At the higher energies there is relatively little angular dependence to  $P_0$  but at the lower energies there are a number of oscillations evident.

An overall view of the phenomenon is seen in Fig. 3 which plots the locations of the peaks ( $n=1, 2, \dots, 7$ ), and valleys ( $n=1\frac{1}{2}, 2\frac{1}{2}, \dots, 6\frac{1}{2}$ ) of  $P_0$  as contours on a plot with axes  $T$  and  $\theta$ . These data bear a strong qualitative resemblance to corresponding plots<sup>2,15</sup> for  $He^+-He$  data.

<sup>14</sup> G. J. Lockwood, H. F. Helbig, and E. Everhart, J. Chem. Phys. 41, 3820 (1964).

<sup>15</sup> D. C. Lorents and W. Aberth, Phys. Rev. 139, A1017 (1965). Their work on  $He^+-He$  extends from 0.015 to 0.600 keV while that of Ref. 2 extends from 0.440 to 225 keV.

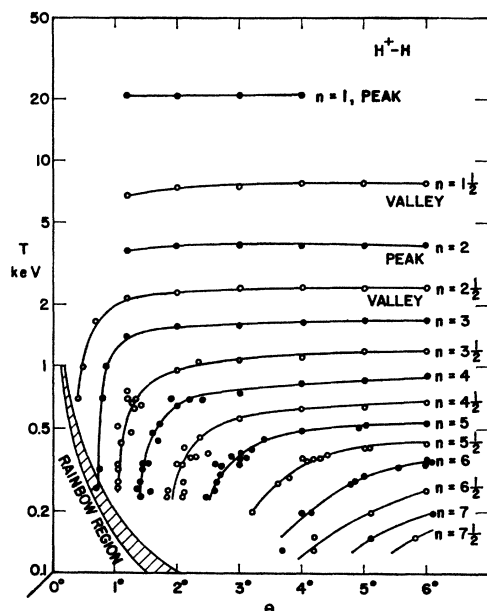


FIG. 3. For  $H^+H$  collisions the locations of the maxima and minima in the electron capture probability  $P_0$  are displayed on axes  $T$  and  $\theta$ , where the incident energy  $T$  is in keV and the laboratory scattering angle  $\theta$  is in degrees. The maxima and minima are identified by indices  $n$  as explained in the text. The data shown in excess of  $3^\circ$  are obtained from equivalent  $D^+D$  collisions.

### b. Empirical Curves

In the figures the solid lines are empirical curves drawn through the data points. In Fig. 1(c) at the low-energy range of the curves for  $1.2^\circ$  and  $2^\circ$  there is considerable data scatter. The reason for this is clear when one refers to the corresponding region of Fig. 3, where it is evident that the points in question lie parallel to the contours. Only a small zero-index error in the angle would cause a large apparent variation in  $P_0$ . The solid lines in Fig. 1 in this case are drawn in a manner to be consistent with the contours of Fig. 3. Greater weight is given to the small-angle data which have the more narrow resolution widths.

### c. $H^+H$ and $D^+D$

The relationship between  $H^+H$  data and the supporting  $D^+D$  data is illustrated in Fig. 2(b). Here 383 eV  $H^+H$  data taken between  $1.3^\circ$  and  $3^\circ$  are compared with 820 eV  $D^+D$  data taken between  $0.7^\circ$  and  $2.7^\circ$ , but this latter is plotted as being equivalent to  $H^+H$  data at 410 eV between  $1.4^\circ$  and  $5.4^\circ$  as has been discussed in Sec. 2b, above. In the first case the  $n=4\frac{1}{2}$  valley is found at  $2.3^\circ$ , and in the second case at  $2.2^\circ$ , these values being equal within the uncertainty of the zero index of the angle scale. In every case where there are data in common the peak and valley locations from the  $H^+H$  results agree with those calculated from equivalent  $D^+D$  data.

### d. Angular Resolution

The effect of angular resolution on the peak heights is best shown in Fig. 2(c), which shows 257 eV  $H^+H$  data with a resolution  $2\Delta\theta$  of  $0.14^\circ$ , 249 eV  $H^+H$  data with a resolution of  $0.6^\circ$ , and 281 eV data (obtained from 562 eV  $D^+D$  collisions) with an effective resolution of  $1.2^\circ$ . The energies being nearly equal, the difference in peak heights may be attributed almost entirely to the differing angular resolutions. The same effect is seen in Fig. 2(b) where a detailed calculation has shown that the peak of the 410 eV curve is raised from 0.75 to 0.83 when a correction is made for the pertinent angular resolution. However, in no case would the peaks be raised to unity nor the valleys lowered to zero by such a correction. Furthermore, angular resolutions effects do not account for damping of the  $P_0$  curves of Fig. 1 in those higher energy regions where the oscillatory phenomenon is largely independent of angle.

### e. Scattered Current versus Angle

The dependence of the current of scattered particles  $I$ , including both protons and atoms, on the scattering angle  $\theta$  gives semiquantitative information on the differential cross section  $\sigma(\theta)$ . It is found convenient to plot  $I\theta^{2.8}$  versus  $\theta T$  as in Fig. 4, which shows data sets taken at several energies below 1 keV. Each of these is normalized to unity at  $\theta T = 0.7$  deg keV. The relationship of these curves to  $\sigma(\theta)$  and to rainbow-angle scattering is discussed below in Sec. 5.

## 4. DISCUSSION

Both the locations of the peaks and valleys of  $P_0$  and their amplitudes are of interest and have been predicted theoretically.

TABLE I. Energies in keV at which maxima ( $n=1, 2, \dots$ ) and minima ( $n=1\frac{1}{2}, 2\frac{1}{2}, \dots$ ) of  $P_0$  occur for  $3^\circ$  scattering of  $H^+H$  as predicted by various authors (a-f) are compared with experimental values.

$n$	Theoretical predictions						Present data
	a	b	c	d	e	f	
1	...	16.9	14.2	19.8	...	...	21.
$1\frac{1}{2}$	...	6.95	5.63	7.50	...	...	7.8
2	...	4.06	3.12	3.88	3.70	6.44	3.9
$2\frac{1}{2}$	2.3	2.70	2.03	2.31	2.30	3.08	2.4
3	1.6	1.96	1.40	1.51	1.55	1.80	1.6
$3\frac{1}{2}$	1.1	1.51	1.03	1.08	1.10	1.183	1.1
4	0.75	...	...	0.80	0.80	0.772	0.78
$4\frac{1}{2}$	0.50	...	...	...	0.61	...	0.58
5	0.30	...	...	...	0.47	...	0.38
$5\frac{1}{2}$	0.10	...	...	...	0.38	...	$\sim 0.15$
6	...	...	...	...	0.31	...	*
$6\frac{1}{2}$	...	...	...	...	0.25	...	*

\* Peak or valley may not exist, as suggested by the contours of Fig. 3.

<sup>a</sup> Francis J. Smith (Ref. 10).

<sup>b</sup> Bates and McCarroll (Ref. 6b) following Ferguson (Ref. 18).

<sup>c</sup> Bates and McCarroll (Ref. 6b) following McCarroll (Ref. 17).

<sup>d</sup> Roth (Ref. 13).

<sup>e</sup> Bates and Williams (Ref. 7).

<sup>f</sup> Mukherjee and Sil (Ref. 8).

### a. Peak and Valley Locations

In its original form the two-state impact-parameter formulation predicted<sup>5,6,16</sup> that the first two peaks should appear at 60 and 6.5 keV, instead of at 21 and 4 keV as observed. Bates and McCarroll pointed out,<sup>6a</sup> and later, drawing on the work of McCarroll<sup>17</sup> and Ferguson,<sup>18</sup> showed quantitatively<sup>6b</sup> that this error in the early theory is largely corrected when proper account is taken of the initial momentum of the electron in the center-of-mass system. Experimentally this phenomenon resulted in a "phase factor" when plotting  $P_0$  versus reciprocal velocity as in the Lockwood and Everhart paper.<sup>1</sup>

Further studies by Bates and Williams,<sup>7</sup> Mukherjee and Sil,<sup>8</sup> and Roth<sup>13</sup> predicted the locations of a number of peaks and valleys of  $P_0$  for  $3^\circ$  scattering. Francis J. Smith<sup>10</sup> derived a rather complete prediction of the peak and valley locations both in energy and angle. Table I presents experimental locations at  $3^\circ$  and compares these with theoretical predictions. Table II gives supplementary experimental data.

It is interesting to note that the characteristic knee of the contours shown in Fig. 3 occurs in the vicinity of  $\theta T = 1$  deg keV. This corresponds to collisions for which, classically, the distance of closest approach is about equal to the radius of the first Bohr orbit. In the limit of large  $\theta T$  the index  $n$  is proportional to reciprocal velocity, the present  $6^\circ$  data fitting fairly closely to the empirical Eq. (6) of Ref. 1 with the same constants found in that paper. Where the contours of Fig. 3 are vertical, then  $n - \frac{1}{2}$  empirically varies with the square

TABLE II. Experimental maxima ( $n=1, 2, \dots$ ) and minima ( $n=1\frac{1}{2}, 2\frac{1}{2}, \dots$ ) of  $P_0$  for  $H^+$ -H collisions are located in energy for three laboratory scattering angles, and in angle for three incident-proton energies. These data supplement  $3^\circ$  experimental values in Table I.

$n$	Turning-point energies (keV)			Turning-point angles (degrees)		
	$1.2^\circ$	$2.0^\circ$	$6.0^\circ$	0.7 keV	0.4 keV	0.25 keV
1	21.	21.	(21.)	†	†	†
$1\frac{1}{2}$	6.8	7.4	7.8	†	†	†
2	3.7	3.8	3.9	†	†	†
$2\frac{1}{2}$	2.2	2.35	2.40	$0.4^\circ$	†	†
3	1.4	1.60	1.7	$0.78^\circ$	$0.70^\circ$	$0.7^\circ$
$3\frac{1}{2}$	0.6	0.97	1.2	$1.3^\circ$	$1.1^\circ$	$1.05^\circ$
4	*	0.64	0.90	$2.2^\circ$	$1.5^\circ$	$1.4^\circ$
$4\frac{1}{2}$	*	0.30	0.69	$>6.0^\circ$	$2.2^\circ$	$1.9^\circ$
5	*	*	0.54	*	$3.2^\circ$	$2.6^\circ$
$5\frac{1}{2}$	*	*	0.43	*	$4.6^\circ$	$3.5^\circ$
6	*	*	0.36	*	*	$4.5^\circ$
$6\frac{1}{2}$	*	*	0.25	*	*	$6.0^\circ$
7	*	*	0.19	*	*	$>6.0^\circ$
$7\frac{1}{2}$	*	*	(0.16)	*	*	*

† Data not taken, angles less than  $0.5^\circ$ .

\* Peak or valley may not exist, as suggested by contours on Fig. 3.

<sup>16</sup> F. P. Ziemba, Ph.D. thesis, University of Connecticut, 1960, p. 37 (unpublished).

<sup>17</sup> R. McCarroll, Proc. Roy. Soc. (London) **A264**, 547 (1961).

<sup>18</sup> A. F. Ferguson, Proc. Roy. Soc. (London) **A264**, 540 (1961).

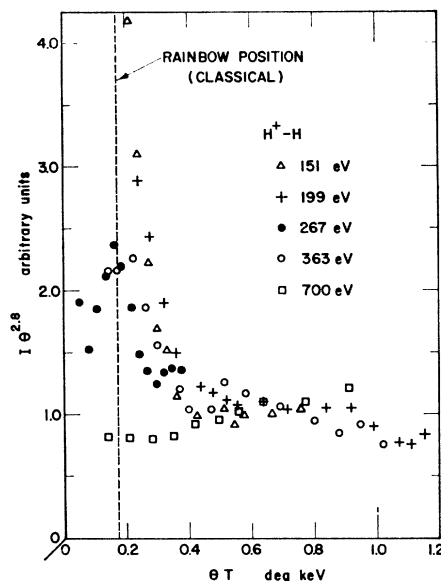


Fig. 4. The product of the scattered-particle current  $I$  (including both ions and atoms) multiplied by the 2.8 power of the laboratory scattering angle  $\theta$  is plotted versus the product  $\theta T$  of angle  $\theta$  and incident ion energy  $T$ . The data shown for 267, 363, and 700 eV are obtained from  $H^+$ -H collisions and those for 151 and 199 eV from equivalent  $D^+$ -D collisions. A dotted line indicates where there is (classically) a discontinuity in the differential cross section. Each set of data points is individually normalized to unity at  $\theta T = 0.7$  deg keV.

root of the angle, as noted also for similar  $He^+$ -He data.<sup>2,3</sup>

### b. Damping

Sections 2e and 5b summarize the experimental situation regarding damping of the  $P_0$  oscillations.

Bates and Williams<sup>7</sup> have accounted for some damping at low energies by extending the impact parameter method to include II states excited by the rapid rotation of the internuclear line. In this connection it is worth noting that Lorents and Aberth,<sup>15</sup> in their study of resonant electron capture at low energies in the  $He^+$ -He system, have been able to study separately the purely elastic collisions, and they observed damping even under these (elastic scattering) conditions. Francis Smith<sup>10</sup> and Marchi and Felix Smith<sup>11,12</sup> have shown that the wave treatment of the charge transfer problem leads to damping even in the two-state (elastic-scattering) approximation.

## 5. RAINBOW-ANGLE SCATTERING

The scattering of protons by atomic hydrogen is largely governed by the potential energies of the two lowest states,  $1s\sigma_g$  (gerade) and  $2p\sigma_u$  (ungerade), of the  $H_2^+$  molecular ion. While the ungerade potential energy is everywhere repulsive, the gerade potential energy changes from attractive to repulsive with decreasing distance. For this potential, classical analysis of the

scattering problem predicts a discontinuity in the differential cross section at a scattering angle  $\theta_R$  given for small angles by  $\theta_R T = 0.17 \text{ deg keV}$ . Ford and Wheeler<sup>19</sup> have shown that the wave treatment of the same problem retains this peculiarity in the cross section although the discontinuity is eliminated. This anomalous increase in the differential cross section, called the "rainbow effect," has been taken into account in the wave treatment by Francis Smith<sup>10</sup> of the charge transfer problem, in the  $\text{H}^+\text{-H}$  collision, and is predicted to influence the  $P_0$  oscillations. For these reasons differential cross section and  $P_0$  data are here taken into the region of  $\theta_R$ .

#### a. Differential Cross Section

The scattered current  $I$  is measured versus  $\theta$  and at high energies is found to vary as  $\theta^{-5}$ . This is the expected result since the Rutherford cross section, applicable when electron screening is negligible, varies as  $\theta^{-4}$  for small angles, the extra factor of  $\theta^{-1}$  arising from the variation of the effective scattering volume with angle. At energies of a few hundred electron volts, where electronic effects become important, it is found that  $I$  varies as  $\theta^{-2.8}$  for angles in excess of  $\theta_R$ . This corresponds to a differential cross section  $\sigma(\theta)$  varying as the inverse  $1.8 \pm 0.2$  power of the angle. The change in cross section behavior in the vicinity of  $\theta_R$  is displayed in Fig. 4, which shows  $I\theta^{2.8}$  plotted versus  $\theta T$  for several energies. Since the ordinates are in arbitrary units and the data for each energy are individually normalized, there is no information here on the absolute value or the energy dependence of  $\sigma(\theta)$ . Instead of  $\theta$ ,

<sup>19</sup>D. W. Ford and J. A. Wheeler, *Ann. Phys. (N. Y.)* **7**, 259 (1959).

the abscissa is chosen to be  $\theta T$  since the classical rainbow angle has a unique position on such a scale, independent of incident ion energy.

The prediction that the differential cross section should increase more rapidly in the vicinity of the rainbow angle is borne out by the data of Fig. 4. In this plot, the 151 eV data show the most pronounced peak. The peak height is smaller for the intermediate energies and no peak is seen for the 700-eV data.

#### b. Rainbow-Angle Effects on $P_0$

Modifications in the locations of the  $P_0$  contours are also predicted<sup>10,12</sup> within the rainbow region. Although a few of the curves in Fig. 2 extend into this region, there are not enough data on the peaks and valleys of  $P_0$  to extend the contours into the shaded rainbow region at the lower left corner of Fig. 3. Lorents and Aberth,<sup>15</sup> who studied  $\text{He}^+\text{-He}$  collisions, found that the oscillations became indistinct and difficult to follow within the rainbow region and this is consistent with our results.

#### ACKNOWLEDGMENTS

We wish to acknowledge the work of Philip Gash, William Keever, and Miss Marianne Melnick who helped take and reduce the data. The continuing interest of Professor Arnold Russek in this work is appreciated. We thank Dr. Grant Lockwood for his part in developing the atomic hydrogen target chamber and establishing experimental procedures. Discussions of the theory with Dr. Francis Smith, Dr. Felix Smith, Dr. Marvin Mittleman, and Professor D. R. Bates have been useful in planning the experiment.